Event-based MPC for propofol administration in anesthesia

A. Pawłowski[1], **M. Schiavo**[2], **N. Latronico** [3], **M. Paltenghi**[4], **A. Visioli**[1]

[1]*Dipartimento di Ingegneria Meccanica e Industriale, University of Brescia, Brescia, Italy*
andrzej.pawlowski@unibs.it, antonio.visioli@unibs.it

[2]*Dipartimento di Ingegneria dell'Informazione, University of Brescia, Brescia, Italy*
schiavo003@unibs.it

[3]*Department of Surgery, Radiology, and Public Health, University of Brescia, Italy*
nicola.latronico@unibs.it

[4]*Spedali Civili di Brescia, Brescia, Italy*
massimiliano.paltenghi@asst-spedalicivili.it

This is the pre-print version of the following article: Event-based MPC for propofol administration in anesthesia, which has been published in final form at https://doi.org/10.1016/j.cmpb.2022.107289.

Abstract: *Background and Objective*: The automatic control of anesthesia is a demanding task mostly due to the presence of nonlinearities, intra- and inter-patient variability and specific clinical requirements to be meet. The traditional approach to achieve the desired depth of hypnosis level is based on knowledge and experience of the anesthesiologist. In contrast to a typical automatic control system, their actions are based on events that are related to the effect of the administrated drug. Thus, it is interesting to build a control system that will be able to mimic the behavior of the human way of actuation, simultaneously keeping the advantages of an automatic system.
Methods: In this work, an event-based model predictive control system is proposed and analyzed. The nonlinear patient model is used to form the predictor structure and its linear part is exploited to design the predictive controller, resulting in an individualized approach. In such a scenario, the BIS is the controlled variable and the propofol infusion rate is the control variable. The event generator governs the computation of control action applying a dead-band sampling technique. The proposed control architecture has been tested in simulation considering process noise and unmeasurable disturbances. The evaluation has been made for a set of patients using nonlinear pharmacokinetic/pharmacodynamic models allowing realistic tests scenarios, including inter- and intra-patient variability.
Results For the considered patients dataset the number of control signal changes has been reduced of about 55% when compared to the classical control system approach and the drug usage has been reduced of about 2%. At the same time the control performance expressed by the integrated absolute error has been degraded of about 11%.
Conclusions: The event-based MPC control system meets all the clinical requirements. The robustness analysis also demonstrates that the event-based architecture is able to satisfy the specifications in the presence of significant process noise and modelling errors related to inter- and intra-patient variability, providing a balanced solution between complexity and performance.

1. Introduction

In total intravenous anaesthesia (TIVA) the main goal is to achieve a desired patient state during surgical intervention addressing three main aspects: analgesia, hypnosis and muscular relaxation. In the traditional approach, the anaesthesiologist manually adjusts the amount of drugs basing on patient's vital signs and on their experience [1]. Due to this, the whole process relies on the human, who can be affected by stress, lack of continuous attention

and tiredness (especially during lengthy interventions) and this can provoke non-optimal drugs dosage [2, 3]. As a consequence, this can lead to postoperative complications originated by under or over dosage of the drug. Some of these issues can be addressed by an automatic control for drug infusion system designed to support the anaesthesiologists in this complex task [1, 2, 4]. From the control system point of view, TIVA is a multiple-input multiple-output (MIMO) system [5]. However, there still exist limitations like the lack of the online pain measure that prevent the design and implementation of the complete MIMO control system [6, 7]. For this reason, most of the closed-loop control systems are focused on the single-input single-output (SISO) problem where only one drug and one controlled variable are considered [3, 8–10]. Alternatively, a MISO (multiple-input single output) approach can be implemented, where the control problem takes into account the drugs coadministration and their resulting effect on a single controlled variable [10, 11]. In this work we focus on a SISO control problem, that is, the depth of hypnosis (DoH) task, where the dosage of the hypnotic drug propofol is the control variable and the Bispectral Index Scale is the controlled variable.

The control systems development for the DoH has attracted the attention of researchers mainly due to its challenging and complex nonlinear nature [5, 12]. Moreover, important effort has been put on Model Predictive Control (MPC), because of its anticipatory character and constraints handling mechanism [13, 14]. The application of MPC techniques to the control of the DoH in the anaesthesia process using propofol has been analyzed in several works, e.g. [12–20]. This interest is motivated mainly by the possibility of predicting the patient response to drug administration [14, 17]. In particular, the methods described in [12, 15] are focused on inter-/intra-patient variability, targeting the most vulnerable aspect in MPC approaches, namely, model uncertainties. These approaches usually results in a complex control system with heavy computational requirements and re-tuning or adaptation is not trivial [20]. From the clinical perspective they are also interesting since they can be used to design personalized control for an individual patient, by exploiting a parameterized patient model based on individual physiological characteristics like gender, weight, height and age to improve the prediction capability [3, 21, 22].

Disregarding the predictive control approach used, most of the mentioned developments are affected by a significant degradation of the control performance when the process noise is considered [11, 17, 23, 24]. The presence of noise in the control system usually results in a noisy control action that, in many cases, implies a non-optimal use of control resources. This problem can be partially addressed by placing a noise filter in the feedback-loop. However, the filtering action needs to be a compromise between noise attenuation and process dynamics modification [22]. Unfortunately, the same problem appears in the DoH control task and this issues is even more critical when the predictive control approaches are used. Taking into account this problem, an event-based control system can be used as a flexible alternative to classic time-based schemes as it can reduce the noise impact on the control action variability providing efficient use of control resources [22, 23, 25]. The application of an event-based paradigm enables the possibility to trigger the controller task basing on the controlled variable dynamics rather than a time progress, which is the main difference when compared to the classical time-based control system. The event-based control approach is an effective and efficient control technique that was already proposed for bioprocesses and energy systems, where the optimal usage of control resources is critical [26]. Usually, these savings in resource usage are made at expense of the control performance, because the event-based control system focuses on keeping the controlled variable within the established limits rather than at a fixed reference value. These properties are also interesting from the DoH perspective in the anaesthesia process. The event-based approach for the DoH was already investigated in [23, 25, 27], where the control system was built using a Proportional-Integral-Derivative (PID) controller and its modification. It was shown that the proposed control approaches are able to reduce the number of control system computations, replicating the anaesthesiologist way of actuation. Event-based MPC controllers are significantly less investigated in context of the anesthesia process. A preliminary study was presented in our previous work [20] where the DoH was considered. Therein, a virtual band on the actuator was imposed and taken into account in the optimization procedure and, consequently, the controlled process was updated in an asynchronous way. The system was verified on one representative patient proving the feasibility of such a method. However, to the authors best knowledge and available bibliographic references, there is no event-based predictive controller with sensor dead-band sampling applied to the DoH in the anaesthesia process. Considering the described potential advantages for the application of event-based control in anaesthesia, a broader hypothesis analyzed in this paper from a clinical point of view is the following: would event-based control reduce the usage of drug thereby improving patient outcomes in terms of recovery and minimal risk for over-dosing?

Taking into account the introduced features and possible benefits, in this paper an event-based MPC control system with dead-band sampling is proposed. Thus, the main contribution of this work consists in the design, development and evaluation under realistic scenario of a predictive event-based control system. The proposed control system exploits a nonlinear pharmacokinetic/pharmacodynamic (PK/PD) patient model for the design of a predictive controller architecture based on the Generalized Predictive Control algorithm. The whole system is based on a previously proposed control system for the DoH [21], where the nonlinear behavior of the DoH process is compensated using the inverse of the nonlinear Hill function. Furthermore, the robustness of the controller is

augmented by the external predictor and an additional filter. In the proposed event-based approach, the control action is updated with a high frequency when the controlled variable goes outside the established tolerance. On the contrary, when the controlled variable remains withing the defined band, the control action is updated with a low sampling frequency, limiting the control effort. Simultaneously, this provides the safety measure that assures the required performance for the closed-loop control system. Thus, the event-based system works with a variable sampling rate, by adapting the controller invocation to the patient DoH represented by the BIS, that is, by adapting the control effort (propofol dosage) to achieve the desired clinical requirements. With this working principle, the control system mimics the anaesthesiologist way of actuation, keeping all the advantages of the closed-loop control at the same time. The designed controller has been extensively tested under realistic scenarios, taking into account real noise extracted from clinical test as well as unmeasurable disturbances. The obtained results are compared with the classic MPC control scheme from [11], which has been designed by explicitly taking into account the noise issue in the DoH control problem. Moreover, the robustness to inter- and intra-patient variability is evaluated by applying a Monte Carlo technique to provide a population wide patients distribution.

The paper is structured as follows. Section 2 is devoted to the propofol PK/PD model description that is exploited in the developed control system. The clinical requirements and control specifications are provided in Section 3. In Section 4, the proposed event-based MPC control architecture is proposed considering the synthesis, the design, the tuning and the implementations aspects. The simulation study used for the evaluation of proposed control system in presented in Section 5. This also includes the inter- and intra-patient variability analysis. Finally, conclusions are summarized in Section 6.

2. Pharmacokinetic-pharmacodynamic model of propofol

The PK/PD model used to describe the patient response to the propofol administration is well known from the literature [28–30]. In particular, regarding the PK, a three compartment mammillary system can be modelled. A state-space model can be derived, where the states are the amount of drug in each modeled compartment. In this case, the input is the drug dosage and the output is the plasmatic concentration, which is proportional to the concentration of the drug in the central blood compartment. The conversion of this model in a transfer function form yields a linear third-order PK term:

$$PK(s) = \frac{C_p(s)}{U(s)} = \frac{1}{V_1} \frac{(s+k_{21})(s+k_{31})}{(s+p_1)(s+p_2)(s+p_3)} \tag{1}$$

where C_p is the plasmatic concentration, U is the propofol infusion rate, p_1, p_2 and p_3 are parameters that depend on the demographics of the patient (age, weight, height, gender), V_1 is the volume of the first compartment and k_{21} and k_{31} represent the flow between the compartments [31]. The PK term is connected in series to the PD part, which consists of a first-order linear system in series with a static nonlinearity (Hill function). The linear part of the PD has the plasmatic concentration as input and the effect site concentration C_e as output and it can be modelled by means of this transfer function:

$$PD(s) = \frac{C_e(s)}{C_p(s)} = \frac{k_{e0}}{s+k_{e0}} \tag{2}$$

where $k_{e0} = 0.456\ [min^{-1}]$.
Finally, the Hill function expresses the relationship between the effect-site concentration and the BIS value. Its expression is [14, 32, 33]:

$$H = E_0 - E_{max}\left(\frac{C_e(t)^{\gamma}}{C_e(t)^{\gamma} + C_{e_{50}}^{\gamma}}\right), \tag{3}$$

where E_0 is the patient's measured value of the BIS before the beginning of the anesthesia procedure, E_{max} is the maximum effect that can be reached by the drug administration, γ is the steepness of the function (in other words, it means the sensitivity of the patient to the propofol), and $C_{e_{50}}$ is the drug concentration that is needed in order to achieve half of the maximal effect.

By grouping the two linear parts $PK(s)$ and $PD(s)$ into one linear term $P(s)$, the system of Figure 1 results, where the propofol infusion rate is the input and the BIS is the process output. Moreover, the intermediate variable, between P and the Hill function block H is the effect site concentration C_e. The resulting model has a Wiener structure and this configuration will be used to build the event-based controls system.

2.1. Patients dataset

The proposed control technique is designed by taking into account the dataset of patients that has been previously exploited for control system design and verification [13, 14, 21]. This dataset is composed of twelve individuals

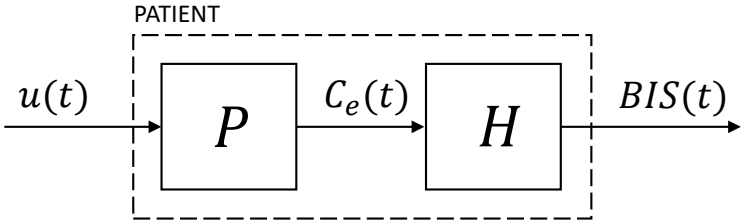

Fig. 1: Patient model with resulting Wiener structure.

but an additional thirteenth patient, determined as the algebraic average of the other individuals, is included. Then, the dataset will be used to analyze intra-patient variability by applying a Monte Carlo technique, while another big dataset will be created to evaluate the inter-patient variability.

3. Clinical requirements and limitations

In the designed event-based control architecture the control variable is the propofol infusion rate and the controlled variable is the desired DoH level, which is measured through the BIS signal. The anesthesia process is divided into two phases. The first one, the induction phase, is a time period necessary to achieve desired level of the DoH from the patient's awake state. Then, the second phase begins. Its the main goal is to maintain the DoH level at the desired range despite the disturbances and it is referred as the maintenance phase. Following the clinical requirements, the desired level of the DoH corresponding to BIS value of 50, should be achieved in approximately 3 minutes in the induction phase. However, this is not a hard constraint and the reference must be reached within 5 minutes to minimize an uncomfortable situation for the patient during intervention. Additionally, in the maintenance phase, the BIS should be kept between 40 and 60. The value should be maintained within the defined range regardless of the process noise and disturbances (mainly originated by nociceptive stimulations). Other limitations that need to be considered are related to the physical limitations and clinical recommendation in the drug dosage system. The physical minimum infusion rate is 0 $[mg/s]$ and represents the non-infusion of the drug. However, following a safety measure applied in the clinical practice, a minimum nonzero baseline infusion u_b should be used. This baseline infusion is used to avoid null values for the drug infusion system even if the value of the BIS is below the desired reference. The baseline infusion for propofol is therefore set to $u_b = 6$ $[mg/kg/h]$ following the recommendation in [34]. Moreover, in the induction phase, the maximum dosage limit is set to 6.67 $[mg/s]$, which originates from the used pump and propofol concentration (*Graseby 3400, Smiths Medical, London, UK* and *Diprivan* 20 $[mg/ml]$). For the maintenance phase the maximum infusion rate is set to 4.00 $[mg/s]$, which reflects the clinical practice for the considered type of the surgery.

4. Event-based MPC control scheme

The proposed control scheme, shown in Figure 2, is based on the predictive control architecture previously presented in [21], which allows the implementation of a personalized control system. It consists of three main components: an event generator, a controller structure and an external predictor [21, 35]. The event generator provides the information for the controller structure when a new control action should be computed due to a new event occurrence. The controller structure consists of a set of feedback GPC controllers, where one of them is selected in accordance with the actual sampling period (time elapsed between two consecutive events). Moreover, the external predictor (composed of $\tilde{P}$, $\tilde{H}^{-1}$ and F_d blocks) is used to compensate the nonlinear element of the patient model, making possible to exploit a linear MPC such as the GPC algorithm. In this scheme, the controlled variable $y(t)$ is the BIS signal, which is monitored continuously with a sampling time T_{base} and the control variable $u(t)$ is the propofol infusion rate, which is updated with a variable sampling time T_f. In such a way, the new control action is computed by the selected controller when a new event is generated. The detailed functionalities and working principle of main components are provided hereafter.

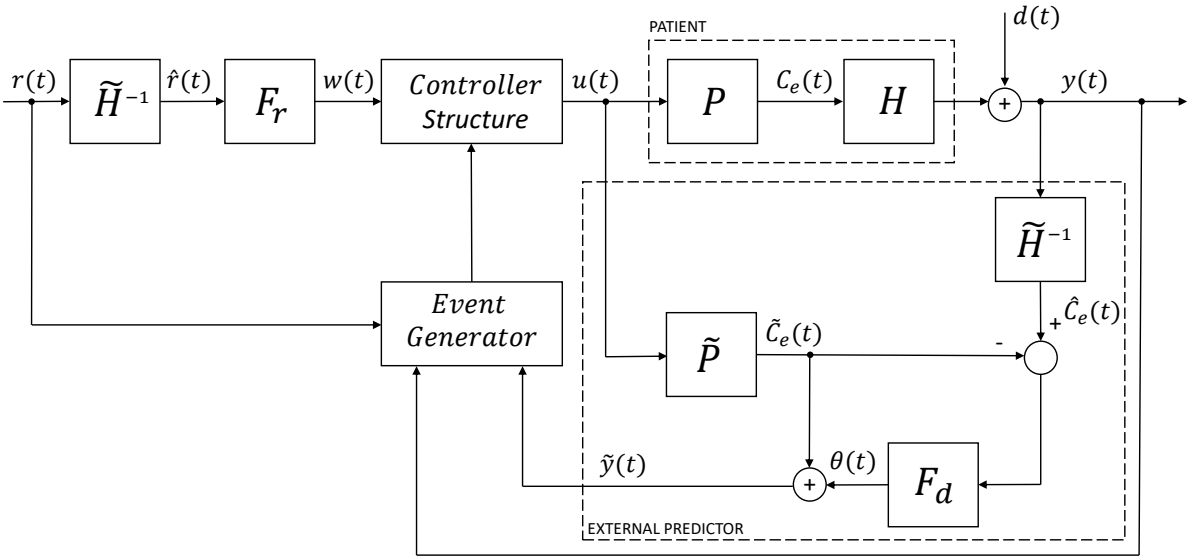

Fig. 2: Event-based control approach for propofol anaesthesia.

4.1. External predictor

The main goal of the external predictor is to compensate for the nonlinear element of the patient model, denoted as $\tilde{H}$. To this end, the inverse of average Hill function $\tilde{H}^{-1}$ is calculated [21]:

$$\tilde{H}^{-1} = C_{e_{50}} \sqrt[\gamma]{\frac{\bar{E} - E_0}{E_0 - \bar{E} - E_{max}}}$$

and is used to relate the BIS and the estimated $C_e(t)$ of the patient (note that $\bar{E}$ refers to the actual BIS measure). In the control architecture, $\tilde{P}$ is the linear part of the PK/PD model of the patient. Its input $u(t)$ is the propofol dosage rate and its output is $\tilde{C}_e(t)$, which is the estimated effect site concentration $C_e(t)$. Then, $w(t)$ is the filtered value of $\hat{r}(t)$, which represents the estimated equivalent effect site concentration for the desired BIS reference value $r(t)$. To obtain the $\hat{r}(t)$ value, the inverse Hill function is employed. Thanks to the application of the external predictor, the control problem is reduced to the linear system that controls the effect site concentration $C_e(t)$ that needs to be achieved for desired BIS level. When the process is affected by modelling uncertainties or by disturbances $d(t)$ (induced by surgical intervention), the difference between the effect site concentration $\hat{C}_e(t)$ obtained from the patient and the effect site concentration $\tilde{C}_e(t)$ obtained from the model is different from zero. This signal signal passes through the first-order low-pass filter F_d, defined as

$$F_d(s) = \frac{1}{T_d s + 1}, \tag{4}$$

which attenuates the effect of disturbances and uncertainties and it is denoted as $\theta(t)$. Finally, the controller structure is used to provide the closed-loop control, where the $w(t)$ value is used as the reference for the set of GPC controllers and the feedback signal is $\tilde{y}(t)$, which contains disturbances from the process. The reference first-order low-pass filter F_r, defined as

$$F_r(s) = \frac{1}{T_r s + 1}, \tag{5}$$

is used to reduce the undershoot in the induction phase and it is designed using a two degree of freedom approach (more details on tuning procedure is provided in Section 4.7).

It needs to be highlighted that predictor blocks are based on an inaccurate PK/PD patient model (since real values are unknown) and in the predictor structure they are denoted with the "˜" mark to clearly differentiate them from the actual ones. More detailed information regarding the compensation scheme can be found in [21].

4.2. Controller Structure

The event-based control scheme shown in Figure 2 has been implemented using the idea introduced in [35] and adapted to control the DoH in anaesthesia process. The proposed architecture operates using the following working principle:

- The BIS signal process output is monitored within a constant sampling period T_{base} at the event generator block, while the control signal update is obtained at an event occurrence time instant and applied to the infusion pump with a variable sampling period T_f, that is, in an asynchronous way.
- T_f is defined as a set of multiple values of T_{base} and results in $T_f = fT_{base}$, $f \in [1, n_{max}]$. Additionally, $T_f \leq T_{max}$, being $T_{max} = n_{max}T_{base}$ the highest sampling period, which is selected to provide a minimum performance for safety reasons.
- For the anaesthesia process T_{base} and T_{max} are defined taking into account clinical practice and specifications.
- Once the control signal is sent to the infusion pump at time instant t, the DoH process state is checked at the event generator block within the base period T_{base}. The event generator block verifies if the controlled variable meets some specific condition and for this the BIS signal is used. When the condition is satisfied, a new event is triggered with resulting sampling period T_f and a new control signal is calculated by the controller. If no events occur, the controlled process is updated in any case after a T_{max} time interval to assure the minimum performance.
- Following the introduced working principle, the controller will compute the control signal using a variable sampling period T_f. Due to this, a set of predictive feedback controllers will be used, each of them designed for a specific sampling period $T_f = fT_{base}, f \in [1, n_{max}]$. Moreover, to avoid adverse bumps during controller commutations, signals resampling techniques are applied.

4.3. Event-based predictive control algorithm

The developed control system uses a model predictive controller exploiting the GPC algorithm. To implement the proposed control architecture, a set of controllers is designed, one for any possible sampling rate T_f. Each GPC controller of the set is implemented and designed using the linear part of the model P (presented in Section2), which is discretized for any sampling rate T_f.

In general, the GPC algorithm provides the control sequence that minimizes the cost function defined as [36]:

$$J = \sum_{j=N_1^f}^{N_2^f} \delta^f [\hat{y}^f(t+j|t) - w(t+j)]^2 + \sum_{j=1}^{N_u^f} \lambda^f [\Delta u^f(t+j-1)]^2 \tag{6}$$

where $\hat{y}^f(t+j|t)$ is a prediction of the system output, $\Delta u^f(t+j-1)$ are increments of control signal and $w(t+j)$ refers to the controller setpoint over the prediction horizon. The GPC tuning parameters are: the minimum and maximum prediction horizons N_1^f and N_2^f, the control horizon N_u^f, the future error scaling index δ^f, and the control weighting factors λ^f [36]. Taking into account that there is no time delay in the process, the value of N_1^f is set to 0 and, consequently, the resulting prediction horizon will be referred as $N^f = N_2^f$ for simplicity. The GPC algorithm provides the future control actions $u^f(t), u^f(t+1), ..., u^f(t+N_u^f-1)$ that will drive the controlled variable $y^f(t+j)$ close to desired reference $w(t+j)$. This is performed by minimizing the J cost function through QP (Quadratic Programming) optimization. During this procedure the constraints of the process are also taken into account during the calculation of the optimal control move.

4.4. Event generator

In the proposed control system, the decision on when new events are triggered is managed by the event generator block shown in Figure 3. This element considers two conditions and when one of them is meet, a new event is triggered. When a new event is generated, the current value of $\tilde{y}(t)$ is send to the control structure with variable sampling rate, forming the y^f vector and a new control value is computed (propofol infusion rate). The first condition is used to monitor the BIS signal and exploits the dead-band sampling method [35], generating a new system event when the absolute value between two variables is bigger than a established interval β. The condition can be formalized as:

$$|r(t) - y(t)| > \beta \tag{7}$$

and detects when the process output, $y(t) = BIS(t)$, differs from the desired set-point $r(t)$, more than a specific threshold β. Note that the controlled variable is $\tilde{y}(t)$; however, it is more natural for the anaesthesiologist to use

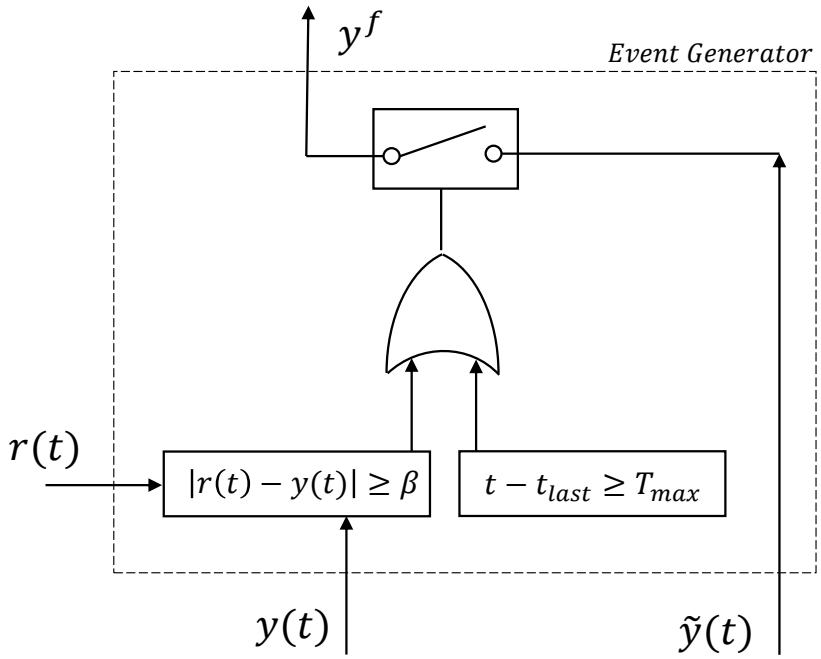

Fig. 3: Event generator block details.

the BIS values, as the threshold for its allowable range is clearly defined, being this the main reason for using this signal for event generation. The second complementary condition is a safety measure, used for minimum performance requirements and is a time-based condition. In this case, the maximum time interval between two consecutive events (between two control signals computation), is given by T_{max}, that is,

$$t - t_{last} \geq T_{max} \tag{8}$$

where t_{last} refers to the time instant when the last event was triggered. Both criteria are verified with the shortest sampling time T_{base}. However, the events are triggered with a variable rate T_f. Finally, the events occurrence will determine the feedback-loop sampling time that will produce the control signal updates in an asynchronous way [35].

4.5. Signal sampling, resampling and reconstruction techniques

As mentioned previously, the calculation of a new control signal is performed in an asynchronous way, with variable sampling rate T_f. Due to this, to execute the GPC algorithm, the past samples of the process output and of the control signal needs to be accessible for each sampling rate T_f. For this, a resampling and reconstruction techniques must be applied for corresponding signals.

- Resampling - Following the introduced working principle, the controller structure block gets the new information from the controlled process only when a new event is triggered. The received data is accumulated in the controller structure element and is resampled to create a base vector y^b that includes the previous samples of the controlled variable with T_{base} rate. This procedure is accomplished by applying a linear interpolation technique among two consecutive signal values. Then, the obtained signal is sampled with the T_{base} frequency and stored. In fact, the $y^b(k)$ vector is created with $k = 0, T_{base}, 2T_{base}, 3T_{base}, \ldots$. After that step, the required samples with past information need to be provided with the new sampling rate T_f, that creates a new vector y^f of past values sampled with T_f rate. Finally, the y^f vector contains the past process data sampled with actual sampling rate T_f and that information is used to compute the next value of the control signal.

- Reconstruction - This procedure is applied to the control signal and is executed in the opposite direction than for the controlled variable. In the proposed scheme, the control signal values are always saved with a T_{base} sampling rate and stored as the u^b vector. In the first step, the required past values are calculated and then the update of u^b is performed. For the new sampling rate T_f, the past information is calculated

using u^b and accumulated in temporary vector u_p^f. Subsequently, the u_p^f and y^f vectors are used to feed the GPC algorithm and to compute the new control signal $u^f(T_f) = u^b(k)$. Finally, the u^b vector is updated by keeping the control action constant among two successive system events.

4.6. Control system constraints

The constraints handling mechanisms is one of the most important advantages of the MPC approach. From the practical standpoint, this is an important feature since it allows all the system limitations to be included during the computation of the control variable, which usually results in a better performance.

Following the information provided in Section 3, the minimum value of the control signal can be defined as $u_{min} = u_b\ [mg/s]$, where u_b refers to baseline infusion for propofol that has been set to $u_b = 6\ [mg/kg/h]$. The saturation of the control variable are defined separately for the induction and maintenance phases and are set to $u_{max} = 6.67\ [mg/s]$ and $u_{max} = 4\ [mg/s]$, respectively. Following the QP formulation, the saturation limits $u_{min} \leq u(t) \leq u_{max}$ are expressed as a set of inequalities on control signal increments:

$$\mathbf{l}u_{min} \leq \mathbf{T}\Delta\mathbf{u} + u(t-1) \leq \mathbf{l}u_{max}$$

where $\mathbf{T}$ is a lower triangular matrix of ones ($N \times N$) and $\mathbf{l}$ is a vector of ones ($1 \times N$). Moreover, the slew-rate infusion pump limitations are directly included in the vector Δu of the control action increments. Such a type of constraints can be represented using the $\Delta u_{min} \leqslant u(t) - u(t-1) \leqslant \Delta u_{max}$ inequality. The vectorial representation is as follows:

$$\mathbf{l}\Delta u_{min} \leqslant \Delta\mathbf{u} \leqslant \mathbf{l}\Delta u_{max}$$

Also these constraints are defined for each anaesthesia phase separately to match the performance requirements. For the induction phase, they are set to have $-1 \leqslant \Delta\mathbf{u} \leqslant 1\ [mg/s]$ and for the maintenance phase $-2 \leqslant \Delta\mathbf{u} \leqslant 2\ [mg/s]$. The aforementioned constraints are implemented as the series of inequalities limiting the controlled variable and are included into the QP optimization problem [21, 36].

4.7. Control system tuning

There are three parameters that are related to the event-based mechanism and that have influence over the control performance: they are the dead-band sampling threshold β, and the T_{base} and T_{max} sampling rates. In the analyzed system, T_{base} has been selected as 1 second and matches the BIS monitor data rate. Then, T_{max} has been set to 10 seconds (that is, n=10) because of safety reasons, as this ensures the minimal performance of the closed-loop control system [11]. Indeed, in a previous work [22], it was shown that the sampling period of 10 second is the maximum value that allows the clinical requirements to be met in terms of accuracy and disturbance compensation capability in the presence of measurement noise. Additionally, the value of β has been fixed to 5. With this threshold, with dead-band sampling and for a BIS reference set to 50, the event-based control system working interval is BIS=50$\pm$5, being inside the desired tolerance for the desired BIS range between 40 and 60 with the necessary safety margins.

Moreover, it is necessary to design the set of GPC controllers to assure the performance defined by the clinical requirements. For this, the GPC parameters need to be tuned. By taking into account the specific requirements, it is worth handling the set-point following and disturbances rejection tasks (that is, the induction and maintenance phases) separately. In fact, from the control system point of view, each of this tasks requires different properties (e.g. disturbance compensation in maintenance phase requires aggressive response of the controller, whereas more conservative tuning is necessary in the induction phase to reduce the undershoot). Due to this, the controller is tuned for maintenance and induction phase separately, applying a two degree-of-freedom approach, that is, dividing the tuning procedure into two stages [37]. At the first stage, the GPC controllers from the set and the F_d filter are designed. During this procedure the parameters N^f, N_u^f, λ^f, and T_d (related, respectively, to the prediction horizon, the control horizon, the control signal weighing factor and the F_d filter time constant) are obtained using a Genetic Algorithm (GA) optimization procedure in order to minimize the performance index defined as Integrated Absolute Error:

$$IAE = \int |r(t) - BIS(t)|dt. \tag{9}$$

Formally, the following cost function is minimized:

$$\min_{N^f, N_u^f, \lambda^f, T_d} \max_{k\in\{1,\ldots,13\}} IAE_k(N^f, N_u^f, \lambda^f, T_d), \tag{10}$$

where $IAE_k(N^f, N_u^f, \lambda^f, T_d)$ refers to the IAE performance measure, calculated from the kth patient of the dataset, and the objective is to minimize the maximum error obtained for all the dataset of the 13 patients. The schematic

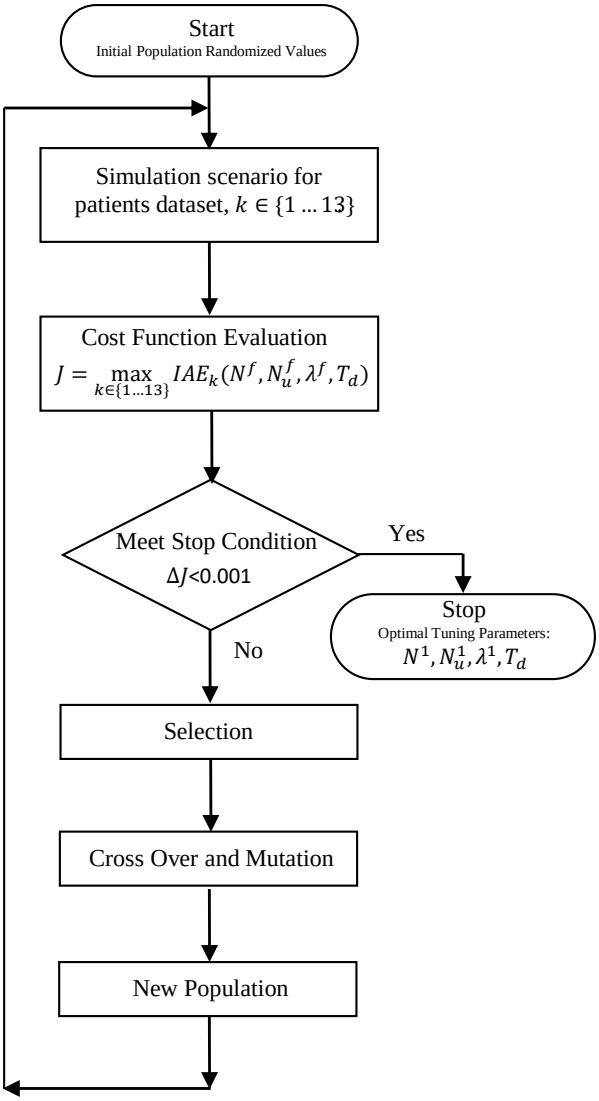

Fig. 4: Schematic chart for the control system tuning using the GA optimization procedure.

chart for the GA optimization task is shown in Figure 4. The tuning procedure is performed applying the design rule for event-based GPC from [35], where the tuning of GPC controller for T_{base} sampling time is used to derive tuning parameters of the remaining controllers from the set. The second tuning stage is focused on the set-point following task and in this case the optimization is simply executed to determine an adequate value of the F_r filter time constant T_r whereas all the remaining parameters are kept the same as for maintenance phase. Additionally, the defined control system constraints were active in both stages of tuning procedure. The resulting control system parameters are summarized in Table 1.

T_{base}	β	n	N^1	N_u^1	λ^1	T_d	T_r
1	5	10	24	2	14.4	47.3	24.6

Table 1: The GPC tuning parameters for T_{base} sampling rate.

5. Simulation results

The performance of the proposed event-based control system is evaluated in simulation to verify that the clinical specifications are met. Simulations have a duration of 20 minutes and include both the anesthesia induction and maintenance phases. The induction phase starts at minute 0 when the BIS set-point $r(t)$ is changed from 100 to the

desired value of 50. Once the BIS target is obtained, the maintenance phase begins. During this phase the ability of the control system to reject disturbances is assessed. To simulate the occurrence of a disturbance on the BIS due to surgical stimuli, a double step signal $d(t)$ is applied [11]. It consists of a positive step of amplitude 10 that occurs at minute 11 of the simulation. It is followed, 5 minutes later, by a negative step of the same amplitude that brings $d(t)$ back to zero, thus simulating the end of the surgical stimuli. The effect of noise is also considered. The noise signal already employed in [22], which has been extracted from real clinical data, is added to the BIS. The noise and disturbance signals are shown in Figure 5. The simulations are performed on the dataset of patients described in Section 2.1. In these first simulations, a perfect knowledge of the linear element of the patient model ($\tilde{P} = P$) is assumed. As regards the Hill function, the average parameters are used instead of the patient's specific ones ($\tilde{H} \neq H$).

To better show the behavior of the event-based control system the first simulation is performed on the average patient of the dataset. The results obtained are shown in Figure 6. The top plot shows the BIS signal, the middle plot shows the propofol infusion rate and the bottom plot shows the behavior of the event generator. In particular, the presence of a vertical line indicates the generation of an event, while its height represent the resulting sampling rate. From the BIS plot it is possible to observe that the clinical specifications are satisfied. Indeed, during the induction phase the BIS reaches the target value in approximately two minutes and during the maintenance phase the BIS is kept close to the target despite the presence of noise and of the double step disturbance. By observing the events plot it appears that the controller generates more events, and thus a shorter sampling rate, in those phases where the BIS is far from the target value. For example, during the induction phase, and between minute 15 and minute 16 when the positive step disturbance occurs and the BIS tends to rise, and between minute 16 and minute 18 when the negative step disturbance occurs and the BIS tends to drop. On the contrary, when the BIS remains close to the target value, less events are generated, with a consequent longer sampling period. For example, between minute 8 and minute 11 the maximum admissible sampling rate of 10 seconds is always selected because the BIS remains close to the target value. The resulting propofol infusion profile is not affected by the presence of residual noise and it resembles the control action typically performed by an anesthesiologist. Indeed, the propofol bolus performed in the induction phase is common in clinical practice and the infusion rate remains constant for long periods of time when the BIS is close to the target. However, the controller promptly responds to significant deviations of the BIS signal from the set-point value.

The simulation is then performed on all the patients of the dataset. The results regarding the induction phase are shown in Figure 7. The BIS target is always reached in less than 4 minutes for each patient of the dataset without undesired undershoots. Only for one patient the BIS falls slightly below 40. This is due to the presence of noise and it is not significant from a clinical point of view. Once the BIS has reached the target it is properly maintained within the recommended range from 40 to 60 despite the presence of noise. The results regarding the maintenance phase are shown in Figure 8. The positive step disturbance occurring at minute 11 is promptly compensated by the controller without causing undershoots. Only for one patient the BIS drops below 40 but it remains above the threshold of 30. Also the negative step is properly compensated.

The event-based control system performance is compared with the classical time-based MPC controller developed in [22], which has been designed to handle the noise in the predictive DoH control system. The performance indexes used for the comparison are the IAE, the integral absolute value of the control action (IAU), defined as:

$$IAU = \int |u(t)|dt, \tag{11}$$

and the total variation of the control action (TV), defined as:

$$TV = \sum_{k=1}^{\infty} |u(k) - u(k-1)| \tag{12}$$

where $u(k)$ and $u(k-1)$ are the values of the control action at two consecutive sampling instants. The TV index is a measure of the control effort and it has been previously used to compare an event-based PID controller with its time-based counterpart [23]. From the anaesthesia process point of view, it is desired to reduce control signal changes especially taking into account the noisy characteristic of the BIS signal used as feedback information. Finally, the total number of events generated is also considered. The results obtained for each patient of the dataset are shown in Table 2. It is worth noting the significant reduction in the number of control signal updates (denoted in the table as events) provided by the event-based controller with respect to the classic time-based controller. In the classic controller they equal the simulation time because they are synchronously generated and they match the sampling period that is equal to 1 second. With the event-based controller the number of control signal updates is reduced from a minimum of 39.3% up to a maximum of 62.2%, with an average reduction of about 54.3%. This is not paid off with a reduction of the control performance as indicated by the IAE. Indeed, with the event-based

Table 2: Performance indexes: comparison between classic time-based controller (Classic) and proposed event-based (EB) for the patients dataset. The Δ value refers to the percentage change of the index taking as the reference the classical time-based system.

	IAE[-]$*10^3$			IAU[mg]			TV[-]			Events[-]		
Patient	Classic	EB	Δ [%]	Classic	EB	Δ [%]	Classic	EB	Δ [%]	Classic	EB	Δ [%]
1	6.49	7.60	17.1	543.7	516.1	-5.1	117.4	115.2	-1.8	1200	574	-52.2
2	8.06	9.15	13.6	563.6	557.8	-1.0	113.4	114.6	1.0	1200	637	-47.0
3	8.07	8.83	9.3	682.2	678.3	-0.6	118.5	101.7	-14.2	1200	501	-58.3
4	5.86	6.95	18.6	549.3	539.9	-1.7	109.4	87.8	-19.7	1200	517	-57.0
5	5.97	6.93	15.9	419.9	405.8	-3.4	86.2	90.5	4.9	1200	566	-52.9
6	7.53	8.70	15.6	637.9	619.3	-2.9	113.0	99.5	-11.9	1200	580	-51.7
7	6.71	7.28	8.5	575.1	555.5	-3.4	114.1	98.9	-13.3	1200	530	-55.9
8	7.54	8.62	14.3	663.2	658.4	-0.7	115.6	100.0	-13.4	1200	534	-55.5
9	10.19	11.56	13.4	566.6	566.4	-0.1	98.9	89.3	-9.8	1200	729	-39.3
10	7.78	8.17	4.9	516.0	504.4	-2.3	78.5	73.8	-5.9	1200	555	-53.8
11	5.69	5.67	-0.4	450.1	437.4	-2.8	94.1	95.2	1.1	1200	454	-62.2
12	5.45	6.02	10.3	451.0	440.0	-2.4	76.2	79.5	4.4	1200	469	-60.9
13	6.93	7.72	11.3	579.8	576.4	-0.6	110.4	99.7	-9.7	1200	484	-59.7
mean	-	-	**11.7**	-	-	**-2.1**	-	-	**-6.8**	-	-	**-54.3**

controller there is a small average IAE increase of 11.7% with respect to the time-based controller. However, this has no relevant deleterious effects on the performance from a clinical point of view. Concurrently, the total amount of drug used (IAU) and the TV are reduced, on average, of 2.1% and of 6.8%, respectively. This indicates that the control action is less subject to unnecessary variations introduced by noise.

5.1. Robustness analysis

A robustness analysis with respect to inter-patient and intra-patient variability is also performed. As regards the inter-patient variability the robustness of the controller over a wide population is assessed. To this end, 500 patients are generated with a Monte Carlo method (MCM). The patient models are generated by randomly selecting the gender, and by using a rectangular distribution of age, height and weight between 18-70 years, 150-190 $[cm]$ and 50-100 $[kg]$, respectively. The Hill function parameters distributions are selected as in [31, 32]. As for the simulation on the dataset, P is set equal to $\tilde{P}$ and $\tilde{H}$ is selected as the average Hill function. The simulation results regarding the induction phase are shown in Figure 9. For each of the 500 patients the BIS target value is reached in less than 3 minutes and the undershoot always remains above the BIS value of 30, thus confirming the satisfactory results obtained on the design dataset. The simulation results regarding the maintenance phase are shown in Figure 10. For each of the 500 patients the double step disturbance is properly compensated without causing undershoots of the BIS below the value of 30 and rises of the BIS above the value of 70. As before, the performance is then compared with that of the classic time-based controller and the results are shown in Table 3. Also in this case the event-based controller provides a reduction of the number of events, of the TV and of the IAU at the expense of a slightly greater IAE.

As regards the intra-patient variability, the robustness of the controller with respect to the mismatches of the linear part of the model is assessed. To this end, for each of the thirteen patients of the dataset, 500 perturbed models P are generated with a MCM on the PK/PD model parameters using the statistical distribution reported in [31], while $\tilde{P}$ is determined by using the average parameters values. So, in this case, we have mismatches both in the linear part of the model ($\tilde{P} \neq P$) and in the Hill function model ($\tilde{H} \neq H$). As an illustrative example, the set-point responses for the 500 perturbed models of the average patient of the dataset are shown in Figure 11. Also in presence of intra-patient variability, the BIS target value is reached in less than 3 minutes and the undershoot always remains above the BIS value of 30. The load disturbance responses for the same set of perturbed models are shown in Figure 12. Also in this case the double step disturbance is properly compensated without undershoots of the BIS below the value of 30 and rises of the BIS above the value of 70. The same results obtained with the perturbed models of the average patient are obtained also for the perturbed models of the others patients of the design dataset as shown in Figure 13 for the induction phase and in Figure 14 for the maintenance phase. Also in case of intra-patient variability, when the performance is compared with that of the classic time-based controller, it appears that the event-based controller provides a reduction of the number of events, of the TV and of the IAU that is paid by a slightly greater IAE, as shown in Table 4. It should be highlighted that the obtained results are important from the clinical practice standpoint since propofol overdosing can lead to undesired effects on the

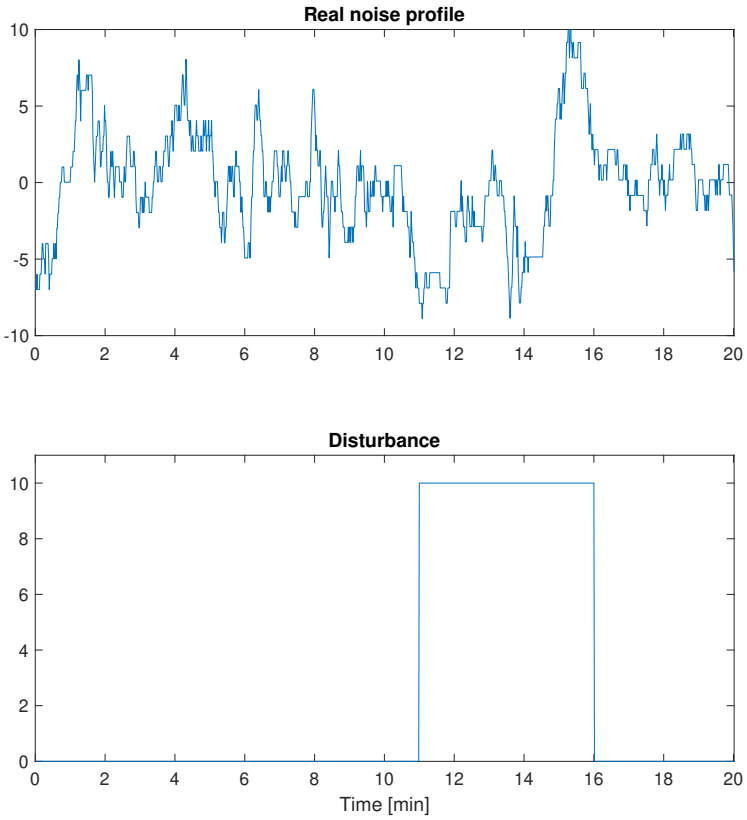

Fig. 5: Noise and disturbance profiles used for simulations.

patient in the form of arterial hypotension and post-operative delirium [38]. In light of these possible problems, it is advantageous to obtain the desired clinical effect (the DoH level) by using a control technique that ensure the correct dosage.

Table 3: Performance indexes for inter-patient variability using mean values for analyzed batch.

	IAE [-]$*10^3$	IAU [mg]	TV [-]	Events [-]
Classic	6.30	459.2	91.0	1200
EB	7.68	443.9	87.3	599
Δ	21.8	-3.3	-4.3	-50.13

Table 4: Performance indexes for intra-patient variability using mean values for analyzed dataset of Patients.

	IAE [-]$*10^3$	IAU [mg]	TV [-]	Events [-]
Classic	7.18	551.4	101.1	1200
EB	8.12	538.7	94.8	567
Δ	13.1	-1.9	-4.9	-52.8

6. Conclusions

In this paper an event-based model predictive control system for depth of hypnosis has been presented. The control architecture employs an external predictor to compensate the nonlinear component of the process and an event-based GPC algorithm with sensor deadband to reduce the variability of the control signal. The proposed system provides a reduction of the number of control signal changes despite the presence of process noise and unmeasurable disturbances. The performance of the analyzed control system has been evaluated using an in-silico study. In realistic conditions, it was possible to reduce the number of control signal changes of about 55% on average.

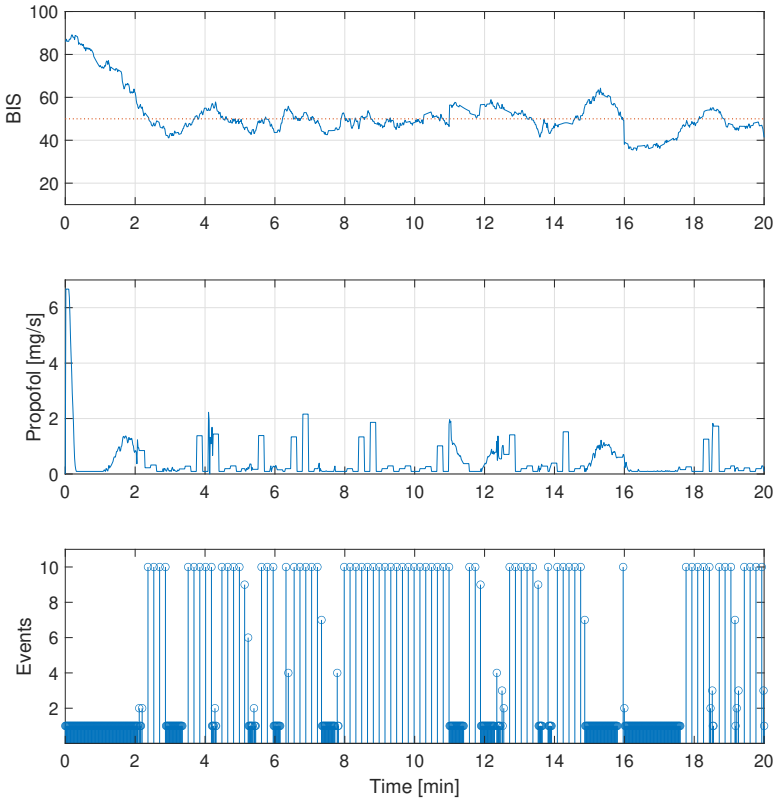

Fig. 6: Results for the average patient 13 using the proposed predictive event-based control system.

On the other side, the control system performance is only 11% less than in the classical time-based framework. Moreover, the proposed event-based approach was able to reduce the amount of the drug used of about 2.1% on average. Taking into account these results, the developed event-based predictive control architecture on the one hand is able to meet the clinical requirements and on the other hand it can reduce significantly the influence of the noise simultaneously saving the control resources (quantity of administrated drug). Additionally, the execution of control actions is similar to the anesthesiologist actuation so that it is likely that this kind of controllers can be more accepted in the clinical practice where the anesthesiologist acts as a supervisor. These findings are important from an interdisciplinary point of view, since the application of the proposed advanced control technique allowed the achievement of the desired performance simultaneously mimicking the human way of actuation.

Acknowledgment

This work has been supported by EU–H2020 funds under MSCA Individual Fellowship - ACTAN project ID: 837912.

References

1. L. Pasin, P. Nardelli, M. Pintaudi, M. Greco, M. Zambon, L. Cabrini, A. Zangrillo, Closed-loop delivery systems versus manually controlled administration of total iv anesthesia: a meta-analysis of randomized clinical trials, Anesthesia and Analgesia 124 (2) (2017) 456–464.
2. A. F. Nimmo, A. R. Absalom, O. Bagshaw, A. Biswas, T. M. Cook, A. Costello, S. Grimes, D. Mulvey, S. Shinde, T. Whitehouse, Guidelines for the safe practice of total intravenous anaesthesia (TIVA), Anaesthesia 74 (2) (2019) 211–228.
3. C. M. Ionescu, I. Nascu, R. D. Keyser, Lessons learned from closed loops in engineering: towards a multivariable approach regulating depth of anaesthesia, Journal of Clinical Monitoring and Computing 28 (2014) 537–546.
4. E. M. Wesselink, T. H. Kappen, H. M. Torn, A. J. C. Slooter, W. A. V. Klei, Intraoperative hypotension and the risk of postoperative adverse outcomes: a systematic review, British Journal of Anaesthesia 121 (4) (2018) 706–721.

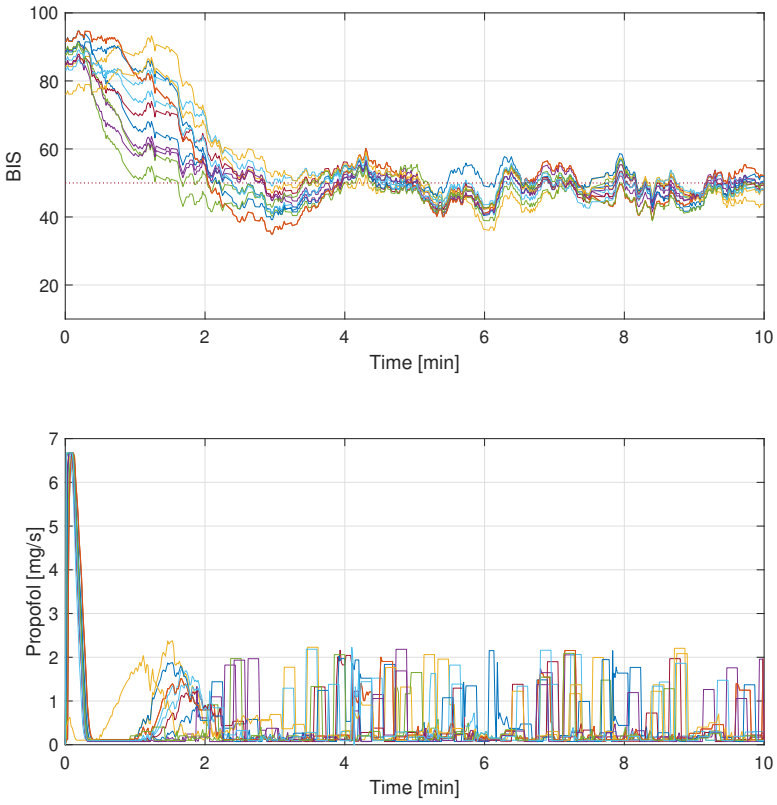

Fig. 7: BIS level and control action in the induction phase for each patient.

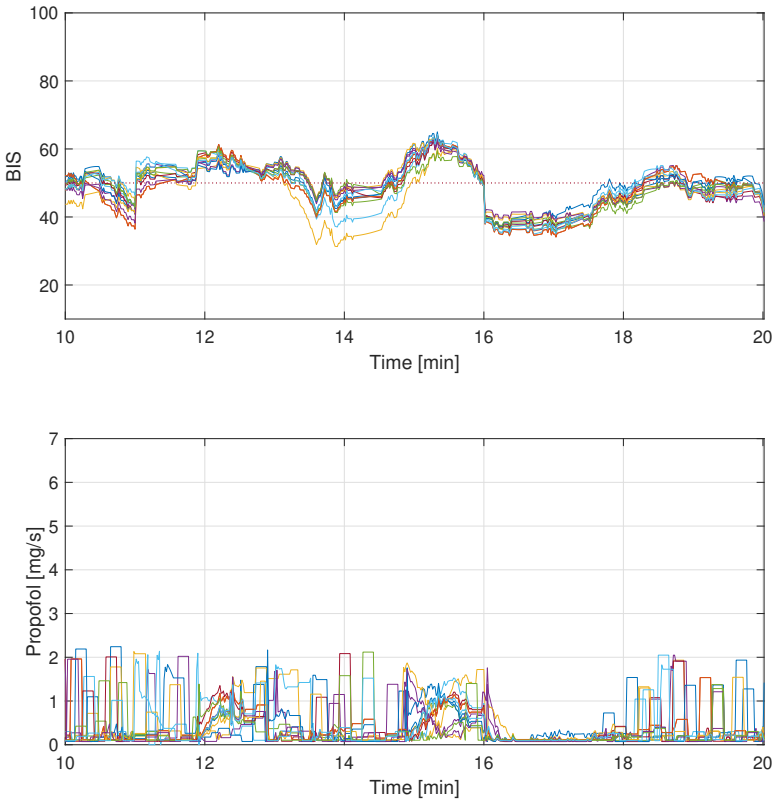

Fig. 8: BIS level and control action in the maintenance phase for each patient.

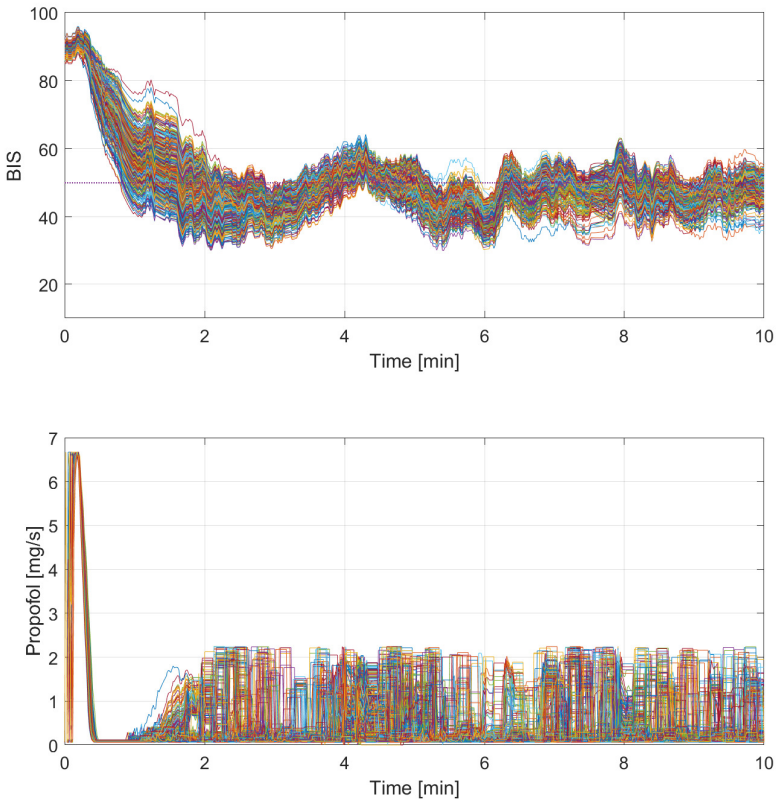

Fig. 9: Set-point step responses by using MCM for inter-patient variability.

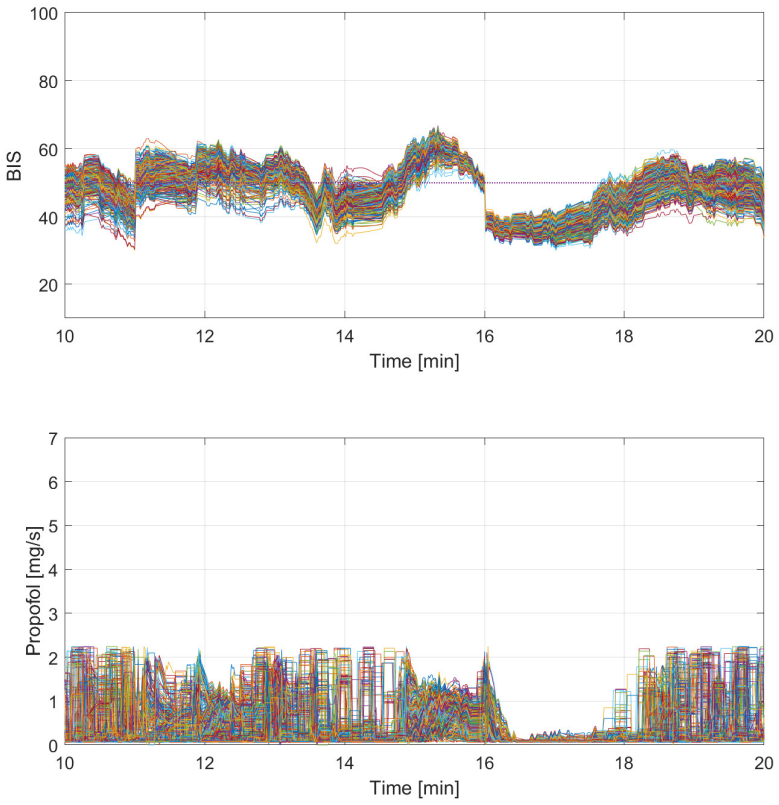

Fig. 10: Load disturbance responses by using MCM for inter-patient variability.

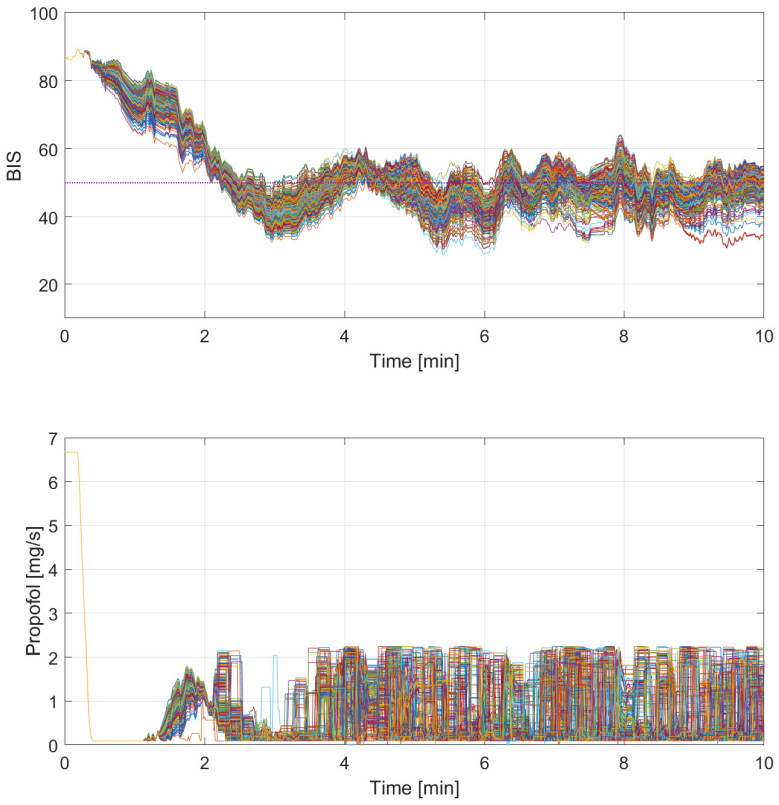

Fig. 11: Set-point step responses for intra-patient robustness (average patient 13).

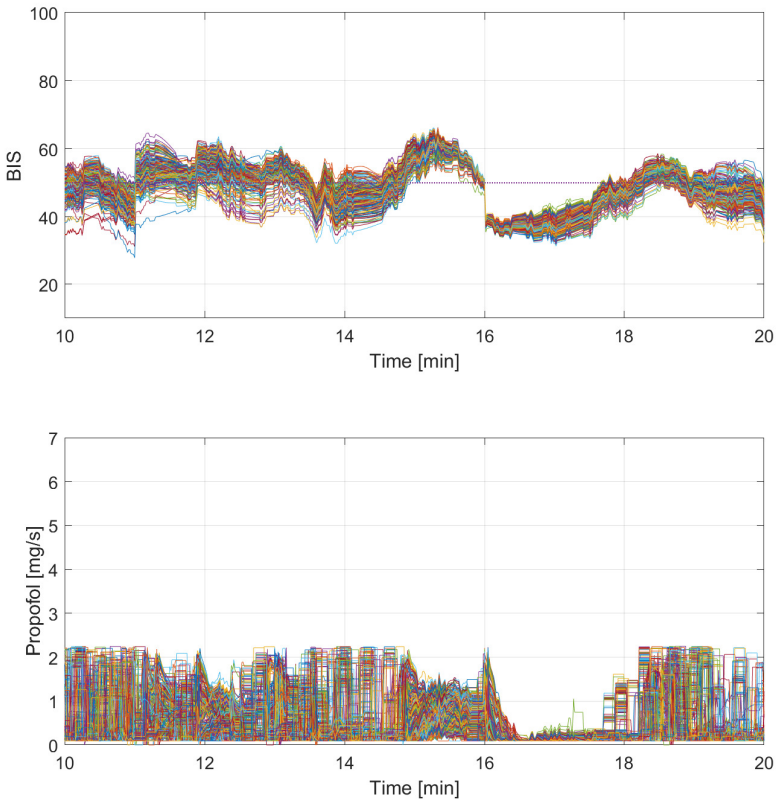

Fig. 12: Load disturbance responses for intra-patient robustness (average patient 13).

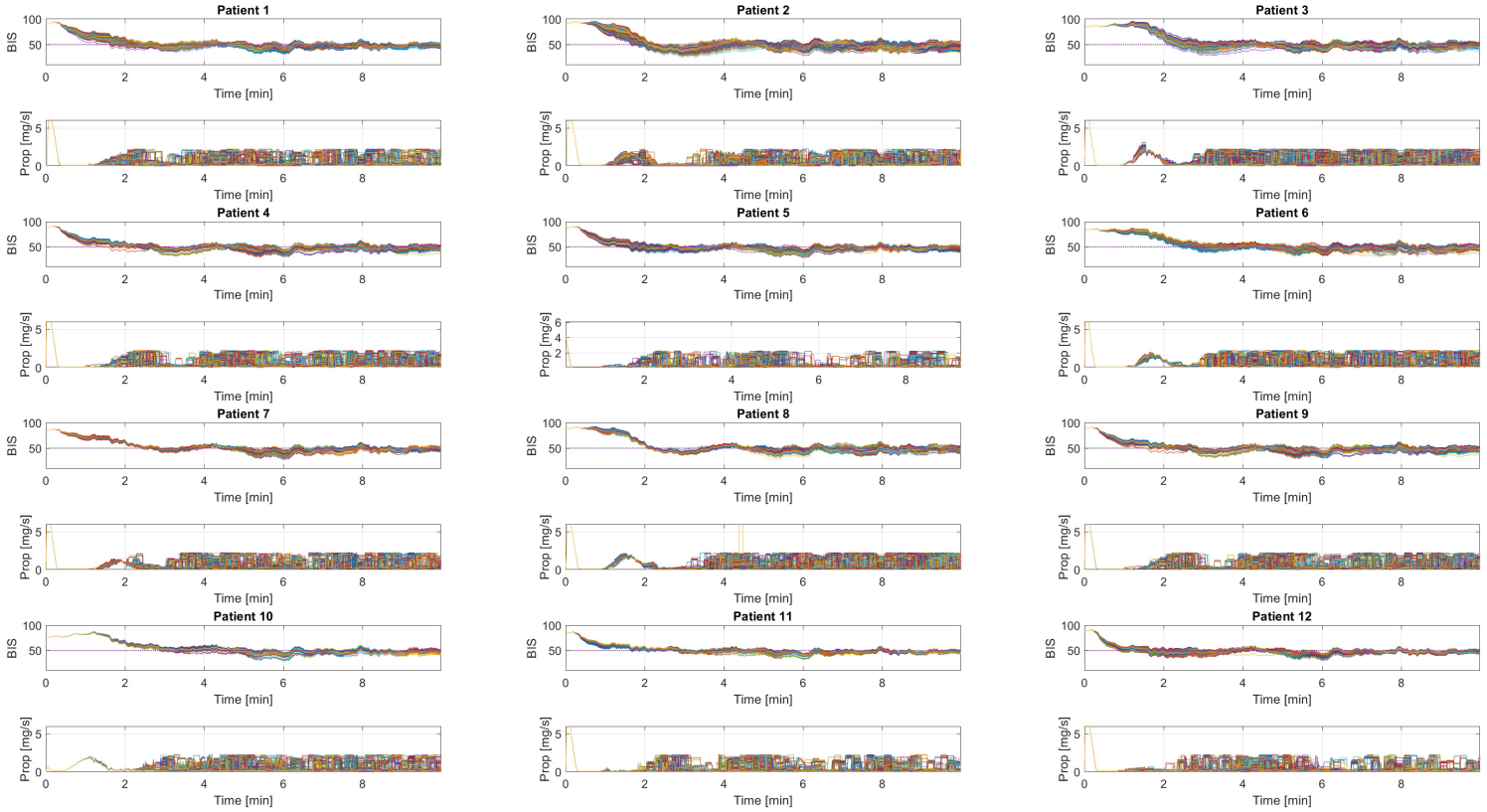

Fig. 13: Induction phase subject to intra-patient variability - simulation results for all the patients of the dataset.

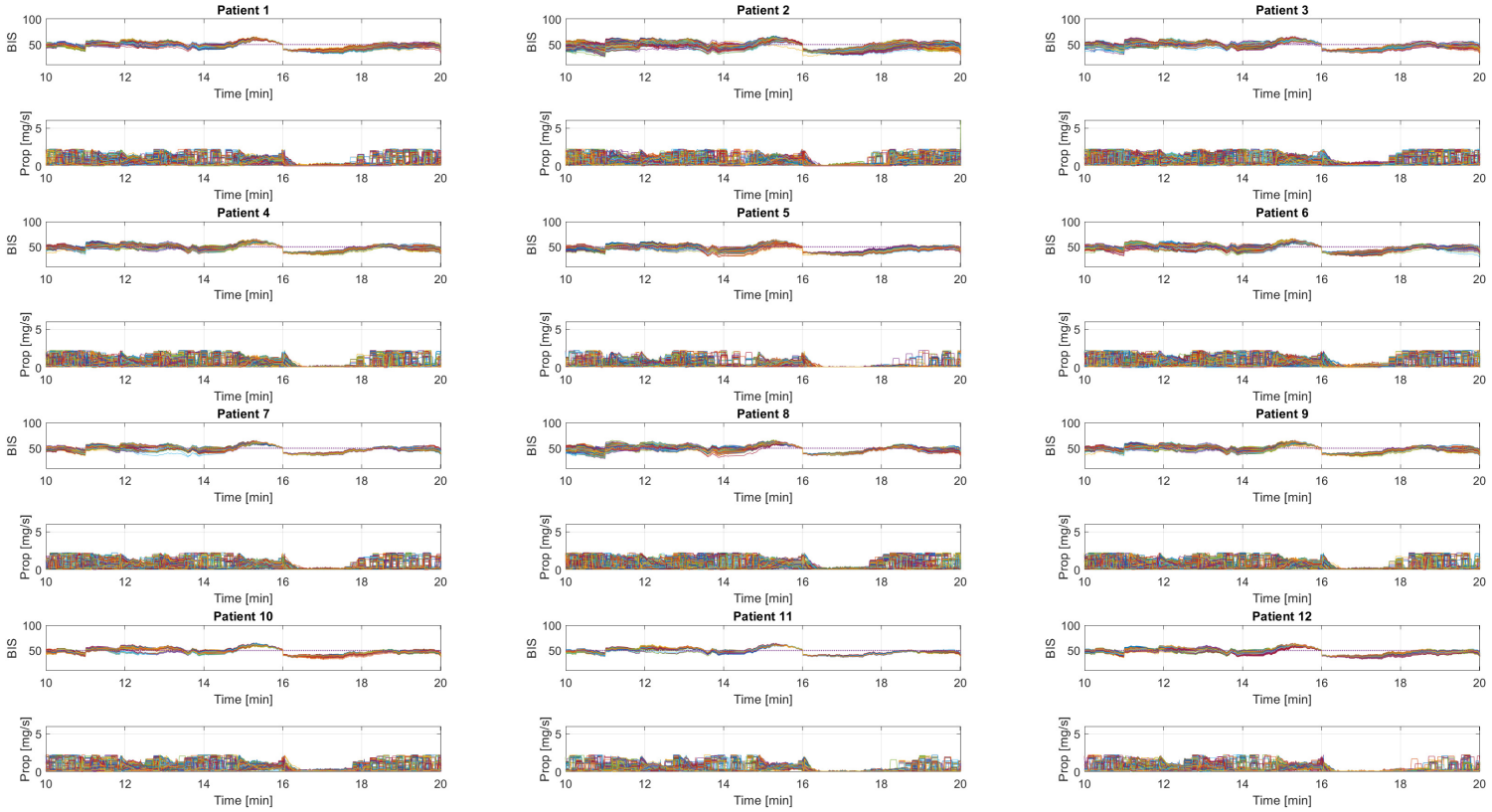

Fig. 14: Maintenance phase subject to intra-patient variability - simulation results for all the patients of the dataset.

5. M. J. Khodaei, N. Candelino, A. Mehrvarz, N. Jalili, Physiological closed-loop control (PCLC) systems: Review of a modern frontier in automation, IEEE Access 8 (2020) 23965–24005.
6. M. Ghita, M. Neckebroek, J. Juchem, D. Copot, C. I. Muresan, C. M. Ionescu, Bioimpedance sensor and methodology for acute pain monitoring, Sensors 20 (23) (2020) 6765.
7. C. Ionescu, M. Neckebroek, M. Ghita, D. Copot, An open source patient simulator for design and evaluation of computer based multiple drug dosing control for anesthetic and hemodynamic variables, IEEE Access 9 (2021) 8680–8694.
8. F. N. Nogueira, T. Mendonca, P. Rocha, Positive state observer for the automatic control of the depth of anesthesia - clinical results, Computer Methods and Programs in Biomedicine 171 (2019) 99–108.
9. J. A. Mendez, A. Leon, A. Marrero, J. M. Gonzalez-Cava, J. A. Reboso, J. I. Estevez, J. F. Gomez-Gonzalez, Improving the anesthetic process by a fuzzy rule based medical decision system, Computer Methods and Programs in Biomedicine 171 (2019) 99–108.
10. N. Eskandari, K. van Heusden, G. A. Dumont, Extended habituating model predictive control of propofol and remifentanil anesthesia, Biomedical Signal Processing and Control 55 (2020) 101656.
11. A. Pawlowski, M. Schiavo, N. Latronico, M. Paltenghi, A. Visioli, Model predictive control using MISO approach for drug co-administration in anaesthesia, Journal of Process Control 117 (2022) 98–111.
12. S. Ntouskas, H. Sarimveis, A robust model predictive control framework for the regulation of anesthesia process with propofol, Optimal Control Applications and Methods 42 (4) (2021) 965–986.
13. I. Nascu, R. Oberdieck, E. N. Pistikopoulos, An explicit hybrid model predictive control strategy for intravenous anaesthesia, Proceedings of the 9th IFAC Symposium on Biological and Medical Systems BMS, Berlin, Germany.
14. C. M. Ionescu, R. D. Keyser, B. C. Torrico, T. D. Smet, M. M. Struys, J. E. Normey-Rico, Robust predictive control strategy applied for propofol dosing using BIS as a controlled variable during anesthesia, IEEE Transactions on Biomedical Engineering 55 (9) (2008) 2161–2170.
15. I. Nascu, E. N. Pistikopoulos, Modeling, estimation and control of the anaesthesia process, Computers and Chemical Engineering 107 (2017) 318–332.
16. I. Nascu, R. Oberdieck, E. N. Pistikopoulos, Explicit hybrid model predictive control strategies for intravenous anaesthesia, Computers and Chemical Engineering 106 (2017) 814–825.
17. A. Krieger, E. N. Pistikopoulos, Model predictive control of anesthesia under uncertainty, Computers and Chemical Engineering 71 (2014) 699–707.
18. Y. Sawaguchi, E. Furutani, G. Shirakami, M. Araki, K. Fukuda, A model-predictive hypnosis control system under total intravenous anesthesia, IEEE Transactions on Biomedical Engineering 55 (3) (2008) 874–887.
19. H. Chang, A. Krieger, A. Astolfi, E. Pistikopoulos, Robust multi-parametric model predictive control for LPV systems with application to anaesthesia, Journal of Process Control 44 (10) (2014) 1538–1547.
20. A. Pawlowski, L. Merigo, J. L. Guzman, A. Visioli, S. Dormido, Event-based GPC for depth of hypnosis in anesthesia for efficient use of propofol, Proceedings of the 3rd International Conference on Event-Based Control, Communication and Signal Processing (EBCCSP), Funchal, Portugal.
21. A. Pawlowski, M. Schiavo, N. Latronico, M. Paltenghi, A. Visioli, Linear MPC for anesthesia process with external predictor, Computers and Chemical Engineering 161 (107747) (2022) 1–13.
22. A. Pawlowski, M. Schiavo, N. Latronico, M. Paltenghi, A. Visioli, MPC for Propofol Anesthesia: the Noise Issue, Proceedings of 6th IEEE Conference on Control Technology and Applications – CCTA 2022, Trieste, Italy, 2022.
23. L. Merigo, F. Padula, N. Latronico, M. Paltenghi, A. Visioli, Event-based control tuning of propofol and remifentanil coadministration for general anaesthesia, IET Control Theory and Applications 14 (2020) 2995–3008.
24. G. A. Dumont, A. Martinez, J. M. Ansermino, Robust control of depth of anesthesia, International Journal of Adaptive Control and Signal Processing 23 (2009) 435–454.
25. L. Merigo, M. Beschi, F. Padula, A. Visioli, A noise-filtering event generator for PIDPlus controllers, Computer Methods and Programs in Biomedicine 355 (2) (2018) 774–802.
26. A. Pawlowski, J. L. Guzmán, M. Berenguel, J. E. Normey-Rico, Event-based GPC for multivariable processes: A practical approach with sensor deadband, IEEE Transactions on Control Systems Technology 25 (5) (2017) 1621–1633.
27. L. Merigo, F. Padula, N. Latronico, T. Mendonca, M. Paltenghi, P. Rocha, A. Visioli, On the identification of the propofol PK/PD model using BIS measurements, Proceedings of the 20th World Congress of the International Federation of Automatic Control, IFAC, Toulouse, France.
28. T. W. Schinder, C. F. Minto, S. L. Shafer, P. L. Andersen, D. B. Goodale, E. J. Youngs, The influence of age on propofol paharmacodynamics, Anesthesiology 90 (1999) 1502–1516.
29. L. Merigo, F. Padula, A. Pawlowski, S. Dormido, J. L. Guzman, N. Latronico, M. Paltenghi, A. Visioli, A model-based control scheme for depth of hypnosis in anesthesia, Biomedical Signal Processing and Control 42 (2018) 216–229.
30. M. M. R. F. Struys, H. Vereecke, A. Moerman, E. W. Jensen, D. Verhaeghen, N. D. Neve, Ability of the bispectral index, autoregressive modelling with exogenous input-derived auditory evoked potentials responsiveness during anesthesia with propofol and remifentanil, Anesthesiology 99 (2003) 802–812.
31. T. W. Schnider, C. F. Minto, P. L. Gambus, C. Andresen, D. B. Goodale, E. J. Youngs, The influence of method of administration and covariates on the pharmacokinetics of propofol in adult volunteers, Anesthesiology 88 (1998) 1170–1182.
32. A. L. G. Vanluchene, H. Vereecke, O. Thas, E. P. Mortier, S. L. Shafer, M. M. R. F. Struys, Spectral entropy as an

electroencephalographic measure of anesthetic drug effect, Anesthesiology 101 (2004) 34–42.
33. C. Ionescu, A computationally efficient hill curve adaptation strategy during continuous monitoring of dose-effect relation in anaesthesia, Nonlinear Dynamics 92 (3) (2018) 843—-852.
34. M. Schiavo, F. Padula, N. Latronico, M. Paltenghi, A. Visioli, A modified pid-based control scheme for depth-of-hypnosis control: Design and experimental results, Computer Methods and Programs in Biomedicine 219 (2022) 106763.
35. A. Pawlowski, J. L. Guzmán, J. E. Normey-Rico, M. Berenguel, A practical approach for generalized predictive control within an event-based framework, Computers and Chemical Engineering 41 (2012) 52–66.
36. E. F. Camacho, C. Bordóns, Model Predictive Control, Springer-Verlag, London, UK, 2007.
37. A. Pawlowski, L. Merigo, J. Guzmán, S. Dormido, A. Visioli, Two-degree-of-freedom control scheme for depth of hypnosis in anesthesia, IFAC-PapersOnLine 51 (4) (2018) 72–77.
38. F. Padula, C. Ionescu, N. Latronico, M. Paltenghi, A. Visioli, G. Vivacqua, Inversion-based propofol dosing for intravenous induction of hypnosis, Communications in Nonlinear Science and Numerical Simulation 39 (2016) 481–494.